On separating propagating and non-propagating dynamics in fluid-flow equations

S. Sinayoko*, A. Agarwal†,
Institute of Sound and Vibration Research, University of Southampton
Z. Hu‡
School of Engineering Sciences, University of Southampton

The ability to separate acoustically radiating and non-radiating components in fluid flow is desirable to identify the true sources of aerodynamic sound, which can be expressed in terms of the non-radiating flow dynamics. These non-radiating components are obtained by filtering the flow field. Two linear filtering strategies are investigated: one is based on a differential operator, the other employs convolution operations. Convolution filters are found to be superior at separating radiating and non-radiating components. Their ability to decompose the flow into non-radiating and radiating components is demonstrated on two different flows: one satisfying the linearized Euler and the other the Navier-Stokes equations. In the latter case, the corresponding sound sources are computed. These sources provide good insight into the sound generation process. For source localization, they are found to be superior to the commonly used sound sources computed using the steady part of the flow.

I. Introduction

Aircraft noise severely impacts the quality of life of residents living near airports and is a problem that will become even more pressing in the future, with air traffic forecast almost to double in the next two decades. One of the most dominant sources of aircraft noise is jet noise. It has been greatly reduced following the advent of high bypass-ratio engines that reduce significantly the jet exit velocity. Further increase in bypass ratio would adversely affect the propulsive efficiency. Hence we need other means of noise reduction. However, despite more than 50 years of research in aeroacoustics, controlling the sound radiated by turbulent jets remains difficult. One reason is that no definite answer has been found on how turbulent flows generate sound.[1] A major obstacle is the lack of understanding of the true sources of sound in a jet.

One way to derive sound sources from a fluid-flow is to use an acoustic analogy. In an acoustic analogy, the complex flow field is first replaced by a simpler flow, in which the propagation of sound is more straightforward. For example, Lighthill's acoustic analogy[2] relies on a quiescent medium, while Lilley's analogy[3] uses a parallel flow. Secondly, an expression for the sound sources is obtained by assuming that the sound propagates through the simpler flow. These sound sources can be used to predict the sound radiating to the far-field. The advantage of the method is to greatly simplify the propagation of sound: complex propagation effects are put within the sources themselves. This is also a disadvantage if we want to identify the true sound source; the sound sources obtained by means of acoustic analogies contain a mixture of the true sound sources, complex propagation effects, and nonlinear hydrodynamic-wave sources present in the original flow. Identifying the radiating core of the source *a posteriori* is very difficult.[4]

An alternative method for identifying the physical sound sources is proposed by Goldstein.[5] He suggests that the governing equations for the acoustic field are the Navier-Stokes equations linearized about the non-radiating flow. The resulting sources depend largely on the non-propagating flow field and because they are devoid of propagation effects and hydrodynamic wave sources, they can be identified as the true

*PhD student, ISVR, University of Southampton
†Lecturer, ISVR, University of Southampton
‡Lecturer, School of Engineering Sciences, University of Southampton

sources of sound. Thus we can compute the sound sources if we are able to separate the radiating and non-radiating parts of the flow. One way to do this is to filter the flow field by means of a linear filter. The filter should remove all the radiating components of the flow, which are those that satisfy the dispersion relation $|\mathbf{k}| = |\omega|/c_\infty$, where $\mathbf{k}$ is the wavenumber, ω the frequency and c_∞ the speed of sound.

However, in subsonic flows, acoustic fluctuations, which travel to the far field at the speed of sound, have a much smaller amplitude than hydrodynamic fluctuations, which are convected with the flow. Also, the acoustic waves interact nonlinearly with the hydrodynamic waves convected with the flow. Also, the acoustic waves interact non-linearly with the hydrodynamic waves. Hence, it is difficult to separate hydrodynamic and acoustic waves in a flow.

The main objective of this paper is to show that it is possible to separate acoustic and non-acoustic fields in fluid-flow equations by using linear convolution filters. The filters we use are problem dependent and are designed based on the physics of the problem – mainly the difference in the dispersion relationship satisfied by the acoustic and hydrodynamic waves. The filtered flow is then used to compute the sound sources. The sound sources based on a non-radiating base flow are easier to interpret physically than those obtained by decomposing the flow-field into its mean and fluctuating parts.

In the next section, we present an expression for aerodynamic noise sources based on a generalised wave equation. We neglect energy sources, thus limiting us to flows where temperature effects are negligible. However, the present work can be extended easily for more general flows. In section III, we show how to construct a non-radiating filter for linearised Euler equations by using a simple example of harmonically excited parallel flow. Then, in section IV, we apply a similar filtering procedure to the Navier-Stokes equations for an axisymmetric jet that is excited at the inflow by two frequencies. The non-radiating base flow is used to compute the corresponding sound sources.

II. Derivation of aerodynamic noise sources

II.A. General source driving small fluctuating quantities in a flow

The definition of fluctuating components is based on filtering the flow field with a linear filter. For a function f, the filtered field $\overline{f}$ is defined by

$$\overline{f} = \mathcal{L}f, \tag{1}$$

where $\mathcal{L}$ is a linear operator. The fluctuating quantities are then obtained by subtracting the filtered quantity from the original one:

$$f' \equiv f - \overline{f}. \tag{2}$$

The aim now is to write the equations governing the evolution of the fluctuating quantities. We start by writing the Navier-Stokes equations:

$$\frac{\partial \rho}{\partial t} + \frac{\partial \rho v_j}{\partial x_j} = 0, \tag{3}$$

$$\frac{\partial \rho v_i}{\partial t} + \frac{\partial \rho v_i v_j}{\partial x_j} + \frac{\partial p}{\partial x_i} = \frac{\partial \sigma_{ij}}{\partial x_j}, \tag{4}$$

where ρ, p and $\mathbf{v} = (v_i)$ denote the density, pressure and flow velocity, and σ_{ij} the viscous stress tensor. Using equation (2), each term in the above equations can be decomposed into a filtered component and a corresponding fluctuating component. If from the resulting equations, we substract the equations obtained by applying the filter $\mathcal{L}$ to equations (5) and (6), we obtain the governing equations for the fluctuating quantities

$$\frac{\partial \rho'}{\partial t} + \frac{\partial (\rho v_j)'}{\partial x_j} = 0, \tag{5}$$

$$\frac{\partial (\rho v_i)'}{\partial t} + \frac{\partial (\rho v_i v_j)'}{\partial x_j} + \frac{\partial p'}{\partial x_i} = \frac{\partial \sigma'_{ij}}{\partial x_j}. \tag{6}$$

Taking $\partial(6)/\partial x_i - \partial(5)/\partial t$ gives

$$\frac{\partial p'}{\partial x_i x_i} - \frac{\partial^2 \rho'}{\partial t^2} + \frac{\partial^2 (\rho v_i v_j)'}{\partial x_i \partial x_j} = \frac{\partial^2 \sigma'_{ij}}{\partial x_i \partial x_j}. \tag{7}$$

We now decompose the non-linear term $(\rho v_i v_j)'$ in equation (7). By making use of Favre average defined by

$$\tilde{f} \equiv \frac{\overline{\rho f}}{\overline{\rho}}, \tag{8}$$

from equation (2), we get

$$(\rho v_i v_j)' = T_{ij} + \rho v_i v_j - \overline{\rho}\tilde{v}_i\tilde{v}_j, \tag{9}$$

where

$$T_{ij} = -\overline{\rho}(\widetilde{v_i v_j} - \tilde{v}_i\tilde{v}_j). \tag{10}$$

Decomposing $\rho v_i v_j$ in terms of filtered and fluctuating components gives

$$\rho v_i v_j - \overline{\rho}\tilde{v}_i\tilde{v}_j = \underbrace{\tilde{v}_i\tilde{v}_j\rho' + \overline{\rho}\tilde{v}_j v_i' + \overline{\rho}\tilde{v}_i v_j'}_{\text{linear terms}} + \underbrace{\rho v_i' v_j' + \tilde{v}_i\rho' v_j' + \tilde{v}_j\rho' v_i'}_{\text{higher order terms}}. \tag{11}$$

The first group of terms on the right hand side of equation (11) consists of linear terms in the fluctuating quantities, whereas the second group is of order two or three in the fluctuating quantities. In particular, the term $\rho v_i' v_j'$ contains the third order term $\rho' v_i' v_j'$. Combining equations (7), (9) and (11) gives

$$\frac{\partial p'}{\partial x_i x_i} - \frac{\partial^2 \rho'}{\partial t^2} + \frac{\partial^2}{\partial x_i \partial x_j}(\tilde{v}_i\tilde{v}_j\rho' + \overline{\rho}\tilde{v}_j v_i' + \overline{\rho}\tilde{v}_i v_j') = \frac{\partial^2 \sigma_{ij}}{\partial x_i \partial x_j} - \frac{\partial^2 S_{ij}}{\partial x_i \partial x_j}, \tag{12}$$

where

$$S_{ij} = T_{ij} + \rho v_i' v_j' + \tilde{v}_i\rho' v_j' + \tilde{v}_j\rho' v_i'. \tag{13}$$

The double divergence of (S_{ij}), denoted by s, can be seen as a source driving the fluctuating quantities:

$$s = -\frac{\partial^2 S_{ij}}{\partial x_i \partial x_j}. \tag{14}$$

Note that we have put the terms which are linear in the fluctuating quantities on the left hand side, and the remaining terms on the right hand side of equation (12). The rationale is that linear terms correspond to propagation effects. Depending on the choice of the filter $\mathcal{L}$, the terms that are nonlinear in perturbations can either be neglected (as small higher order terms), or can act as acoustic sources. This will become clear in the following subsections. Also, we have left the viscous stress tensor out of S_{ij}, because it is generally responsible for dissipating waves rather than generating them.

An underlying assumption has been made here regarding the source definition. The definition implies an absence of back reaction from the fluctuating quantities to the source.

II.B. Source associated with a steady baseflow

A traditional way of decomposing the flow is to use a time average filter. For a given position $\mathbf{x}$ and time t, the time-averaged filtered quantity $\overline{f}(\mathbf{x}, t)$ is given by

$$\overline{f}(\mathbf{x}, t) = f_0(\mathbf{x}) = \lim_{T\to+\infty} \frac{1}{T}\int_0^T f(\mathbf{x}, \tau)\, d\tau, \tag{15}$$

where f_0 denotes the associated mean flow quantity.

In such cases, the fluctuating components are essentially of two kinds:

$$f' = f_h + f_a, \tag{16}$$

where f_h corresponds to hydrodynamic waves and f_a to acoustic waves, assuming that such a decomposition is possible. The hydrodynamic waves are convected with the flow, while the acoustic waves travel at the local speed of sound. The associated source term s is responsible for driving both hydrodynamic and acoustic waves.

If one is interested in the source of sound, problems might arise from the realization that the source s, based on the steady flow, also includes some propagation effects. This can be illustrated by considering

the nonlinear terms in fluctuations on the right hand side of equation (13). For example, $\rho v_i' v_j'$ can be decomposed as

$$\rho v_i' v_j' = \rho(v_{ia} v_{ja} + v_{ia} v_{jh} + v_{ih} v_{ja} + v_{ih} v_{jh}). \tag{17}$$

Here, the term that is nonlinear in acoustic quantities, $v_{ia} v_{ja}$, will be small and can be neglected. The term $v_{ih} v_{jh}$ would be a source term for both acoustic and hydrodynamic perturbations. The remaining terms that are linear in the acoustic field are propagation terms that should be transferred to the left hand side because they modify the medium in which the acoustic waves propagate. This is an example of a source that drives both acoustic and hydrodynamic waves. It is not clear how one would separate the sources that drive the acoustic field from those that drive the hydrodynamic field. One way to overcome this problem is investigated in the following subsection.

II.C. Source associated with an unsteady silent baseflow

Let $\mathcal{L}$ be a filter that removes all acoustic components of the flow field. Hence, $\overline{f}$ becomes non-radiating (silent base flow), and the fluctuating component f' is only made of acoustic waves:

$$f' = f_a. \tag{18}$$

In other words, the filter removes the radiating acoustic components of the flow, while leaving the mean and hydrodynamic components unchanged. In the rest of the paper, the filters which ensure that the base flow does not contain any radiating acoustic components will be called *non-radiating filters*. Filters which remove radiating acoustic components from the base flow while leaving the mean and hydrodynamic components unchanged will be referred to as *optimal non-radiating filters*.

In the source region, the acoustic fluctuations are several orders of magnitude smaller than the mean and hydrodynamic fluctuations. In particular, the high-order terms in equation (13) are negligible compared to T_{ij}. For an optimal non-radiating filter, in the source-region, the source term reduces to

$$s \approx -\frac{\partial^2 T_{ij}}{\partial x_i \partial x_j}. \tag{19}$$

II.D. Non-radiating filter

In the frequency domain, the filtered quantity is obtain by Fourier transforming $\overline{f}$:

$$\overline{F}(\mathbf{k}, \omega) = \int_{-\infty}^{+\infty} \int_S \overline{f}(\mathbf{x}, t) e^{i(\omega t - \mathbf{k}\cdot\mathbf{x})} \, d^2\mathbf{x} \, dt, \tag{20}$$

where $(\mathbf{k}, \omega)$ is the frequency-domain coordinate system. Goldstein[5] showed that, for an unbounded turbulent flow through a quiescent medium, if the filter $\mathcal{L}$ is such that

$$\overline{F}(\mathbf{k}, \omega) = 0 \quad \text{when} \quad |\mathbf{k}| = |\omega|/c_\infty, \tag{21}$$

then $\mathcal{L}$ is non-radiating, i.e. $\overline{f}$ does not contain any radiating acoustic components.

If in addition to being non-radiating, $\mathcal{L}$ is such that $\overline{f}$ contains all the mean and hydrodynamic components, leaving only acoustic radiating components in f', then $\mathcal{L}$ is an optimal non-radiating filter. Non-radiating filters are highly desirable because, as shown in section II.C, they lead to an unambiguous expression of the sound sources.

Differential filter

Obtaining a non-radiating filter in the time-domain is desirable because it could be implemented easily within explicit time-domain methods. One such filter is the d'Alembertian operator, defined by

$$\Box^2 = \frac{1}{c_\infty^2} \frac{\partial^2}{\partial t^2} - \nabla^2. \tag{22}$$

If $\overline{f} = \Box^2 f$, then it can be shown that

$$\overline{F}(\mathbf{k}, \omega) = \left(|\mathbf{k}|^2 - \frac{\omega^2}{c_0^2} \right) F(\mathbf{k}, \omega), \tag{23}$$

which proves that $\overline{F}$ satisfies equation (21). The d'Alembertian filter can be used directly in the time domain, using equation (22), or by windowing in the frequency domain, using equation (23).

Another important feature of differential filters is that they are local. In reality, the source of sound is also local, i.e independent of what may occur away from the point of interest. This issue was raised by Jordan et al.[1] and is a critique directly applicable to convolution filters.

Convolution filters

Convolution filters are of the form $\overline{f} = w * f$, where

$$\overline{f}(\mathbf{x}, t) = \int_{-\infty}^{+\infty} \int_{\mathcal{V}} w(\mathbf{y}, \tau) f(\mathbf{x} - \mathbf{y}, t - \tau) \; d\mathbf{y} \, d\tau, \tag{24}$$

where w is a function defining the behaviour of the filter and $\mathcal{V}$ denotes the entire spatial domain. These filters use information from the entire signal f, which gives more flexibility to extract the desired features from f. In addition, from the convolution theorem, we have

$$\overline{F}(\mathbf{k}, \omega) = W(\mathbf{k}, \omega) F(\mathbf{k}, \omega), \tag{25}$$

where $\overline{F}$, W, and F are respectively the Fourier transforms of $\overline{f}$, w and f. Convolution filters can therefore be conveniently applied as windowing operations in the frequency domain. For signals that involve large sets of data, this is more efficient than using equation (24).

The problem is then to define an appropriate window W in the frequency domain, that renders the corresponding filter w non-radiating. For a non-radiating filter, the window $W(\mathbf{k}, \omega)$ should go to zero whenever $|\mathbf{k}| = |\omega|/c_\infty$, i.e

$$W(\mathbf{k}, \omega) = 0 \quad \text{if} \quad |\mathbf{k}| = \frac{|\omega|}{c_\infty}. \tag{26}$$

An additional requirement for an optimal non-radiating filter is that

$$W(\mathbf{k}, \omega) = 1 \quad \text{when} \quad |\mathbf{k}| \neq \frac{|\omega|}{c_\infty}. \tag{27}$$

As noted by Goldstein,[5] it is impossible to satisfy both equation (26) and (27), because the part of the window where it should go to zero would be infinitely small. In practise, it is sufficient to satisfy equation (27) for the main hydrodynamic components of the flow when there is a clear separation from the acoustic components in the $\mathbf{k} - \omega$ plane.

One example of a non-radiating filter is

$$W(\mathbf{k}, \omega) = \left[1 - \exp\left(-\frac{(|\mathbf{k}| - |\omega|/c_\infty)^2}{2\sigma^2} \right) \right]. \tag{28}$$

This is equal to one almost everywhere, except around components satisfying the dispersion relation, where it goes to zero. The width of the region over which the window goes from one to zero is approximately equal to 2σ. The above filter is close to optimal for small values of σ.

An alternative method for defining a non-radiating filter is to focus on capturing the main hydrodynamic components of the flow. A prior understanding of the hydrodynamic content of the flow is required to do so. Such understanding can be obtained by a careful analysis of the Fourier transform of the flow field.

III. Filtering a two-dimensional parallel shear layer flow

III.A. Problem description and implementation

This problem is from the *Fourth Computational Aeroacoustics Workshop on Benchmark Problems*.[6] The shear layer is described in two-dimensions as a parallel flow, with a prescribed velocity profile. The shear layer models a hot jet of Mach number $M = 0.756$. A harmonic Gaussian source, of frequency $\omega_s = 76$rad/s, is located at the origin. It generates acoustic waves and excites an instability wave. The flow pressure is of the form

$$p = p_0 + p_h + p_a, \tag{29}$$

where p_0 is the mean pressure, p_h the excited instability wave and p_a the acoustic waves.

The solution is obtained by solving the Linearised Euler Equations (LEE) using an explicit finite-difference scheme. The spatial derivatives are obtained by a Dispersion-Relation-Preserving scheme.[7] The solution is integrated in time using a fourth-order six-step Runge-Kutta scheme. The grid is uniform in both directions. The computational domain is defined by

$$-70 \leq x \leq 600, \quad N_1 = 1200, \tag{30}$$

$$0 \leq y \leq 150, \quad N_2 = 903, \tag{31}$$

where N_1 and N_2 are the number of grid points in the x and y directions. A thick buffer zone is used downstream, for outflow boundary condition, to avoid reflections from the outer boundaries. The buffer is an extension of the zonal characteristic boundary condition developed by Sandberg and Sandham.[8] The buffer contains 800 points. Such a large buffer is required to avoid the contamination of the physical domain by reflections originating from the exit boundary condition. Small buffers are also used on the other sides of the computational domain to allow acoustic waves to exit the domain without reflections.

The pressure component is filtered by two filters. First of all, the d'Alembertian filter of equation (22) is applied at every time step to obtain $\Box^2 p$. Secondly, the solution p is written over 5 periods $T_s = 2\pi/\omega_s$, using 125 time frames, in order to compute the filtered solution in the frequency domain. Instead of filtering out the acoustic waves directly, we use a Gaussian window centred around the instability wavenumber k_0,

$$W(\mathbf{k}, \omega) = \exp\left[-\frac{(k_x - k_0)^2}{2\sigma^2}\right] + \exp\left[-\frac{(k_x + k_0)^2}{2\sigma^2}\right], \tag{32}$$

where k_x is the streamwise wavenumber, $k_0 = 0.68\text{m}^{-1}$ and $\sigma = 0.1\text{m}^{-1}$. The corresponding filtered pressure is denoted by $\mathcal{G}p$.

III.B. Results

The pressure field $p(x,t)$ is plotted in figure 1(a). The figure shows the presence of two kinds of waves radiating from the origin: acoustic waves radiating to the far-field, and hydrodynamic waves growing in the downstream direction along the x-axis. Figures 1(b) and 1(c) show the filtered pressure obtained by using respectively the d'Alembertian filter $\Box^2$ and the Gaussian filter $\mathcal{G}$. A comparison between p and $\mathcal{G}p$ along the line $y = 15\text{m}$ is presented in figure 1(c).

III.C. Discussion

Figures 1(b) and 1(c) clearly show that both d'Alembertian and Gaussian filters render the pressure field non-radiating. However, the d'Alembertian filter changes the structure of the hydrodynamic waves. This is a direct consequence of the fact that equation (27) is not satisfied by the d'Alembertian operator.

On the contrary, the base flow obtained by using the Gaussian filter is in very good agreement with the original flow in the region where the instability wave is dominant. This is shown qualitatively by comparing figures 1(a) and 1(c). This suggests that the Gaussian filter is optimal. To confirm this, the filtered pressure $\mathcal{G}p$ is compared along the line $y = 15$ in figure 1(d) to an exact solution of the hydrodynamic part of the flow, obtained by Agarwal et al.[9] The agreement is very good.

Thus, filtering in the frequency domain gives sufficient flexibility to obtain an optimal non-radiating filter.

IV. Sources of sound in an axisymmetric jet flow

IV.A. Problem description

In this section, we filter a flow simulated by a DNS of a fixed axisymmetric mean flow excited at the inflow by two frequencies. The frequencies are chosen to trigger some instability waves in the flow. These instability waves grow downstream and interact non-linearly, thereby generating acoustic waves. There is some evidence, from Sandham et al.,[10] that non-linear interaction is a significant source of aerodynamic noise in subsonic jets. In this section, we filter the flow by means of an optimal non-radiating filter, in order to identify the sources of sound in the jet.

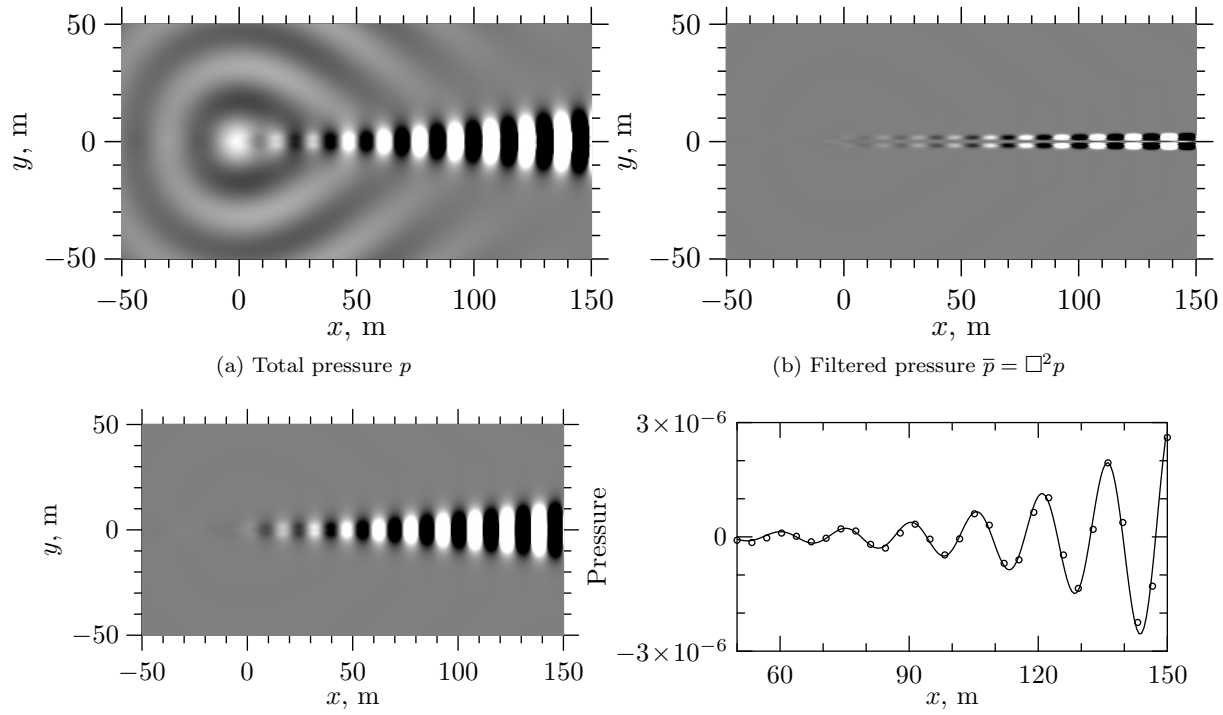

(a) Total pressure p

(b) Filtered pressure $\overline{p} = \Box^2 p$

(c) Filtered pressure $\overline{p} = \mathcal{L}$

(d) Profiles of hydrodynamic pressure (solid line) and pressure $\mathcal{G}p$ (circles), along $y = 15$

Figure 1: Comparison of total pressure p with the filtered pressure obtained by applying the d'Alembertian operator $\Box^2$, and the Gaussian filter $\mathcal{L}$. In the pressure plots, the contour scale is linear and extends from $-5 \cdot 10^{-5}$Pa (black) to $5 \cdot 10^{-5}$Pa (white).

The main flow characteristics are as follows. The Mach number is 0.9 and the Reynolds number is 3600. The base mean flow is chosen to match the experimental data of Stromberg *et al.*[11] The mean flow is axisymmetric and the radial and azimuthal components of the mean velocities are set to zero. The excitation modes excited at the two unstable frequencies are also axisymmetric. The flow is adiabatic so that the theory of section II.A is applicable.

This case is one of several carried out by Suponitsky and Sandham,[12] who have run simulations with different combinations of excitation frequencies and amplitude. The data used here corresponds to the simulated case with the largest acoustic radiation. The two excitation frequencies are $\omega_1 = 2.4$ and $\omega_2 = 3.4$, where the frequencies are normalized by jet exit velocity and jet diameter. The flow was obtained by solving the compressible Navier-Stokes equations. The spatial derivatives were carried out by using a fourth-order central difference scheme, and time integration was performed with a third-order explicit Runge-Kutta scheme. Entropy splitting of the inviscid flux terms was used to enhance the numerical stability of the code.

IV.B. Flow analysis

All the results are normalized by jet diameter D, jet exit velocity U and far-field density.

Figure 2 shows the fluctuating part of the presssure field, i.e $p - p_0$ where p_0 is the mean pressure, in the upper part of the physical domain. The domain extends over 22 jet diameters in the streamwise direction, and 30 jet diameters in the transverse direction. The figure clearly shows hydrodynamic waves propagating along the jet axis and acoustic waves radiating to the far field.

More information can be gained by studying the power spectrum of the pressure field both in the source region and in the far field. The power spectra corresponding to the pressure signal measured at $(10, 0)$ and $(10, 10)$ are shown in figures 3(a) and (b), using thick lines. From figure 3(a), the two dominant frequencies along the jet axis are the excitation frequencies $\omega_1 = 2.2$ and $\omega_2 = 3.4$. Non-linear interaction also generates some waves at the difference frequency $\Delta\omega = 1.2$, with a smaller amplitude (-10dB compared to the waves

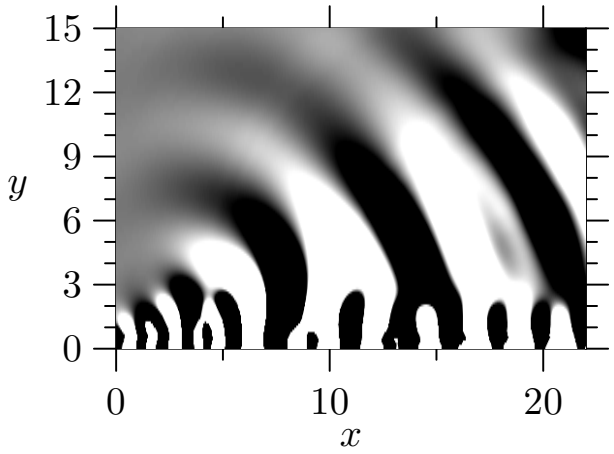

Figure 2: Fluctuating part of pressure $p - p_0$. The contour scale is linear and extends from $-5 \cdot 10^{-6}$ (black) to $5 \cdot 10^{-6}$ (white).

of frequency ω_1). Higher harmonics can be seen at frequencies $2\omega_1 = 4.4$ and $2\omega_2 = 6.8$, as well as the interaction frequency $\omega_1 + \omega_2 = 5.6$. However, these higher frequencies have a much smaller amplitude.

Further away from the axis, where the acoustic field dominates, it can be seen from figure 3(b), that the flow is dominated by the difference frequency $\Delta\omega = 1.2$. The next significant components are $\omega_1 = 2.2$ and $\omega = 0.6$, with an amplitude reduced by 20dB compared to the dominant frequency.

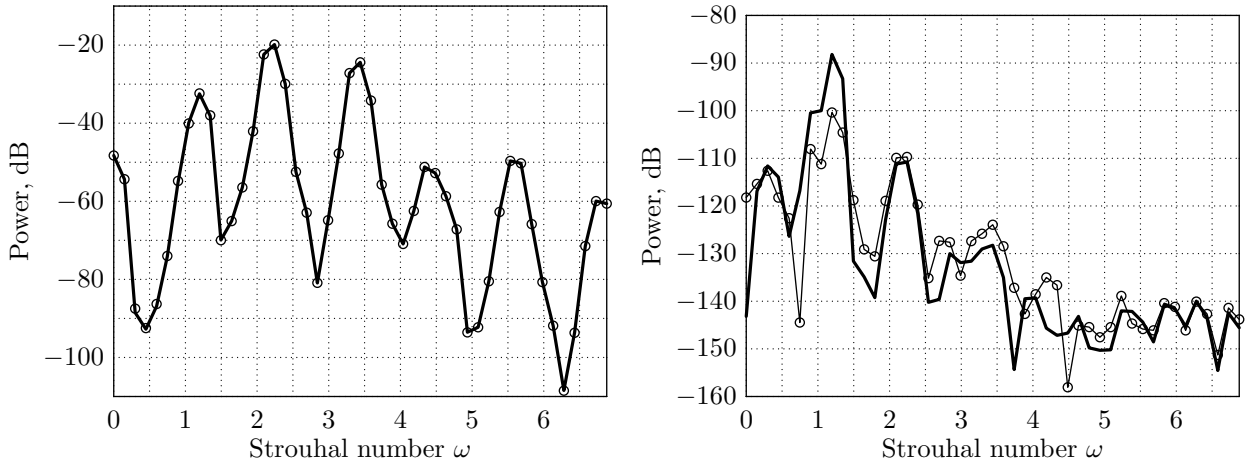

(a) $(x, y) = (10, 0)$ (b) $(x, y) = (10, 10)$

Figure 3: Examples of pressure power spectra along the jet and in the acoustic region. The excitation frequencies are $\omega_1 = 2.2$ and $\omega_2 = 3.4$. The acoustic field is dominated by the interaction frequency $\Delta\omega = 1.2$. The thick lines correspond to the flow pressure p and the thin lines with circles to filtered pressure $\overline{p}$.

IV.C. Flow filtering

We have shown that the acoustic field is dominated by frequency $\Delta\omega = 1.2$. We therefore design a filter which removes the wavenumber components $|\mathbf{k}| = \Delta\omega/c_\infty = 1.09$. The filter is a convolution filter g applied in the frequency domain, and defined by the window

$$W(\mathbf{k}, \omega) = \frac{1}{2}\left[1 + \tanh\left(\frac{|\mathbf{k}| - k_0}{\sigma}\right)\right], \tag{33}$$

where $k_0 = 1.3$ and $\sigma = 0.2$. The filter can be expressed in the time domain, for any flow component f with mean f_0, as

$$\overline{f} = f_0 + g * (f - f_0). \tag{34}$$

A first indication of the filter efficiency at removing acoustic components and maintaining hydrodynamic ones from the flow is given in figures 3(a) and (b), where the power spectra of p and $\overline{p}$ are plotted for two different points. The plot in figure 3(a), shows that the frequency content of p and $\overline{p}$ is identical along the jet axis, which is what we expect. On the contrary, in the acoustic region, figure 3(b) shows a reduction of 10dB at the frequency $\Delta\omega$, which is the principal acoustic frequency. The filter seems to be able to reduce the acoustic radiation significantly, while preserving the hydrodynamic features of the flow. This is investigated further by looking at instantaneous plots of the pressure fields, as well as pressure profiles along the jet axis and within the acoustic region.

The filtered pressure $\overline{p}$ and fluctuating pressure $p' = p - \overline{p}$ are plotted, for a single time-frame, in figure 4. Comparing figures 4(a) and 2 shows that the filtered pressure component contains no acoustic waves at frequency $\Delta\omega$. Some higher frequency waves can however be seen. These correspond to weak Mach waves at frequencies ω_1 and ω_2. The sound generation mechanism for Mach waves is linear and is well understood. We would like to identify the non-linear sound source mechanisms and we chose to leave the Mach waves in the base flow. The effectiveness of the filter can be clearly seen from the fluctuating pressure field p' in figure 4(b) that contains only the acoustic waves. This is true even in the source region. This is remarkable considering that these waves are at least an order of magnitude smaller than hydrodynamic waves. Moreover, this figure indicates that the source of sound, at this particular time, is somewhere between 2 and 5 jet diameters.

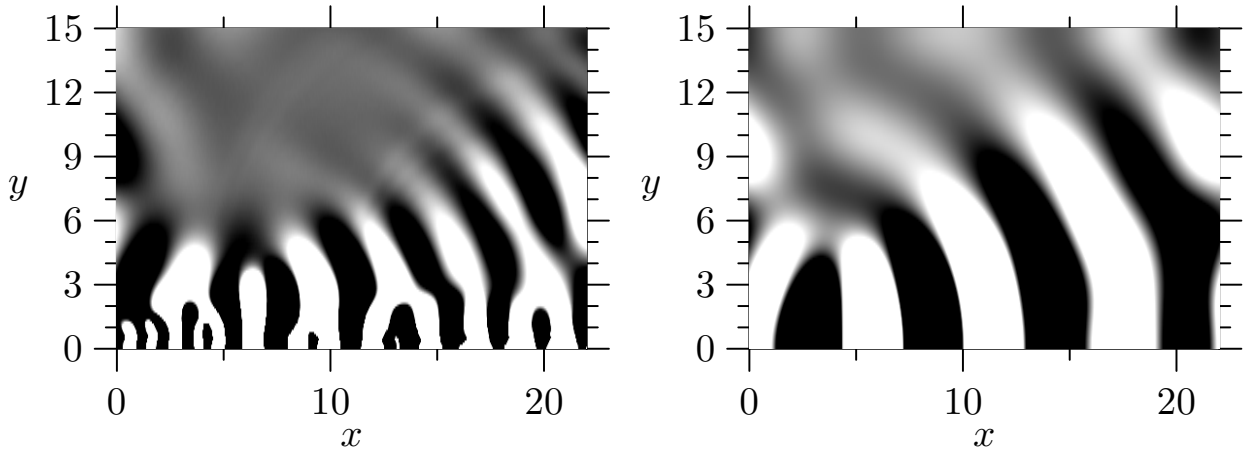

(a) Filtered pressure $\overline{p}$ (b) Fluctuating pressure $p' = p - \overline{p}$

Figure 4: Filtered pressure and fluctuating pressure fields for a single time frame, obtained by applying the filter of equations (33) and (34). The filter is non-radiating and is optimal: $\overline{p}$ contains no radiating acoustic components (other than Mach waves), and p' is composed only of acoustic waves.

The filter has also been validated by examining some pressure profiles in both the near-field, where the hydrodynamic field dominates, and along a sideline where the acoustic field dominates. For an optimal filter, $\overline{p}$ should be almost identical to p, because radiating acoustic waves are of a smaller order of magnitude. Figure 5 confirms that this is the case. In the acoustic region, p' should be equal to the acoustic components of the flow, expressed as $p - p_0$. Figure 5 shows that this is true, at least within the range $2 \leq x \leq 10$. The difference can be explained, for $x < 2$, by errors introduced by Fourier transforms near the edges, and for $x > 10$ by the presence of Mach waves. These difference should not have major consequences for our purpose of identifying the sources of sound in the jet, for which, from section II.D, we need to compute $\overline{p}$ accurately in the near field, which is easier than computing p', the latter being more sensitive to numerical errors.

IV.D. Sources of sound

Results

The sources associated with the non-radiating filter defined in the previous section and the time-averaging procedure of section II.B, are computed using equation (13). In the case of the non-radiating filter, the

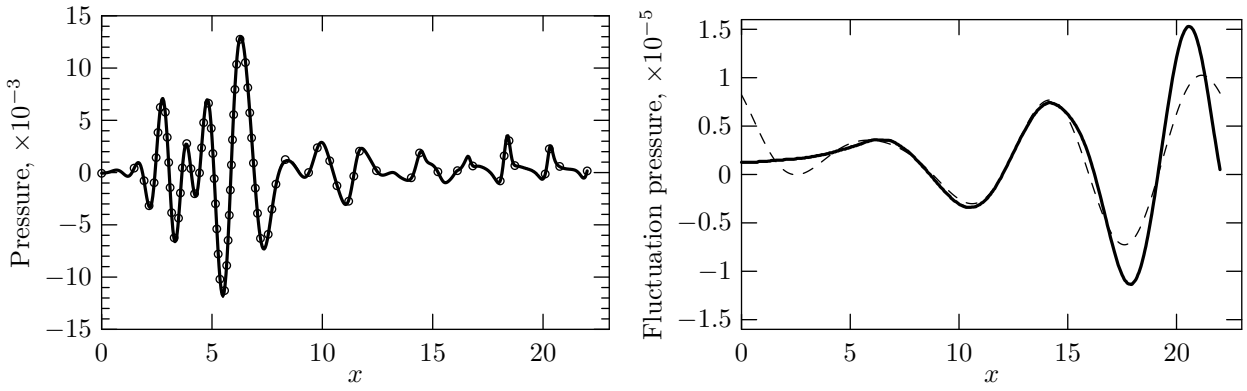

(a) Source region, $y = 0$

(b) Far field, $y = 10$

Figure 5: Pressure profiles along the jet axis ($y = 0$) and in the source region ($y = 10$). On figure (a), the filtered pressure $\overline{p}$ (circles) is compared to the pressure p (solid line). On figure (b), the fluctuating pressure p' (dashed line) is compared to the unsteady part of pressure $p - p_0$ (solid line).

fluctuating components are negligible compared to the other terms and the source definition simplifies to equation (19).

Figures 6(a) and (b) show the corresponding source fields close to the jet exit for $0 \leq y \leq 2.5$ at a single time frame. The jet mixing layer corresponds to $y = 0.5$. Figure 6(a) shows the source obtained by using a steady base flow, and figure 6(b) the one associated with the non-radiating filter introduced in the previous subsection.

To analyse more finely the frequency content of the source, the power spectrum of each source is plotted at points chosen differently for each source, so that they are centred in a region where the magnitude of the source is significant, based on figures 6(a) and (b). For the steady base flow source, the chosen point is $(x, y) = (5.5, 0.5)$. The point corresponding to the silent base flow source is $(x, y) = (4.5, 0.4)$. The two power spectra are plotted in figure 6(c) and (d).

Discussion

As shown in figure 6(a), the steady base flow source is spread out over the entire jet mixing-layer, for $x \geq 2$. It consists mostly of high wavenumber structures. A slightly larger feature can be seen around 5.5 jet diameters. The spectrum corresponding to this particular location, on figure 6(c), shows a peak frequency at $\omega = 1.2$. This suggests that this point might correspond to a source of sound. However, the source also contains all of the frequency components observed in the original flow, for example $\omega_1 = 2.2, \omega_2 = 3.4$, but also $2\omega_1 = 4.4$, $\omega_1 + \omega_2 = 5.6$ and $2\omega_2 = 6.8$. The amplitude of all these waves is roughly the same and is less than 10dB below the peak frequency at $\Delta\omega = 1.2$. One should note, however, that this result does vary depending on the position of the point used to plot the power spectrum. At other locations, $\Delta\omega$ is not the peak frequency. Thus, although the far-field pressure consists mostly of waves at the frequency $\Delta\omega$, this is not the case for the source term.

The source term associated with the silent base flow, shown in figure 6(d), is very different. It is also located in the jet mixing-layer, but only between 0 and 5 jet diameters. From figure 4(b), this is precisely the region from where sound seems to be originating. The source term has an interesting quadrupole-like shape. Note that the centre of this source is actually oscillating back and forth in time. The spectrum shows a peak close to the interaction frequency $\Delta\omega = 1.2$. Other frequencies are present, but at more than 15dB below the peak level (apart from $\omega = 0.6$ which is only a bit more than 5dB below). Quite remarkably, the three dominant frequencies shown in this power spectrum, i.e $\Delta\omega = 1.2$, $\omega = 0.6$ and $\omega_1 = 2.2$, are the same as the three frequencies dominating the far-field pressure, as shown in figure 3. Although the nature of the peak frequency $\omega = 0.6$ remains unclear, this is a good indication that the source obtained by using an unsteady silent base flow is likely close to the true source of sound.

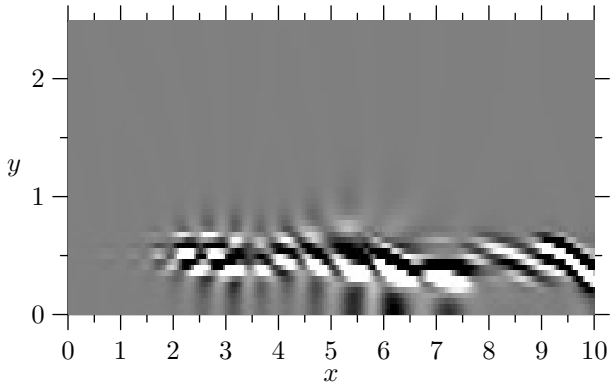

(a) Sound source s for time-averaged base flow. The contour scale extends from $-5 \cdot 10^{-2}$ (black) to $5 \cdot 10^{-2}$ (white).

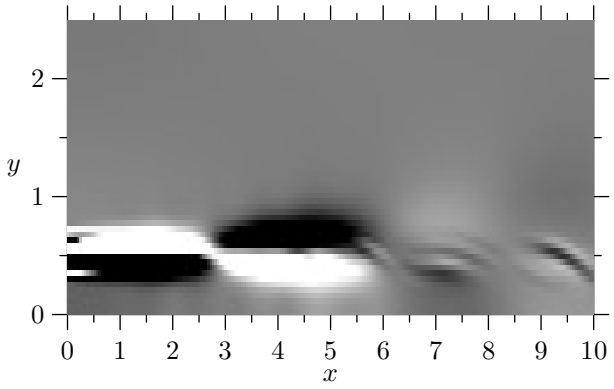

(b) Sound source s for non-radiating base flow. The contour scale extends from $-5 \cdot 10^{-3}$ (black) to $5 \cdot 10^{-3}$ (white).

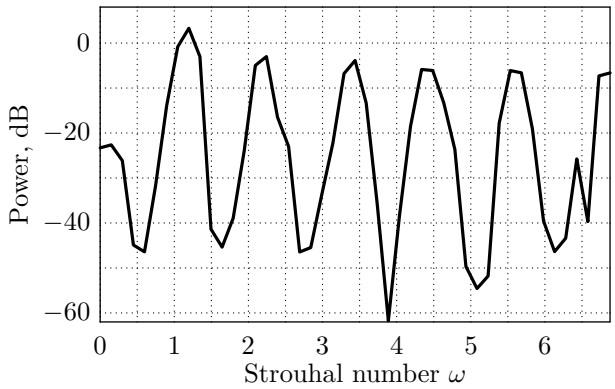

(c) Source spectrum at position $(x, y) = (5.5, 0.5)$ for a time-averaged base-flow.

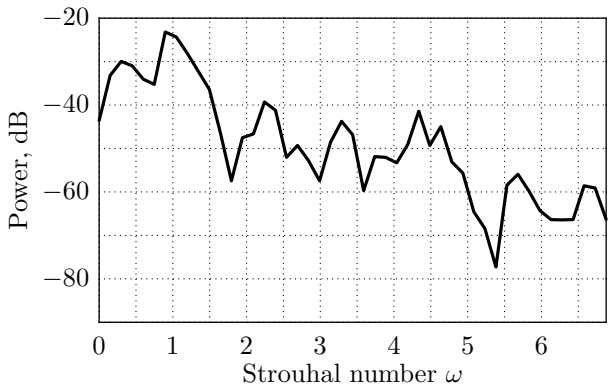

(d) Source spectrum at position $(x, y) = (4.0, 0.4)$ for a non-radiating base-flow.

Figure 6: Sound sources based on a time-average filter (figure (a)) and a non-radiating filter (figure (b)). The power spectrum for those two sources is plotted in figures (c) and (d) respectively.

V. Conclusions and future work

A formal procedure leading to a new definition of the sound sources has been developed. The formulation is similar to the one by Goldstein[5] but leads to a single source expressed as the double divergence of tensor. Energy source terms are not taken into account. The source is based on a base flow containing all non-radiating components of the flow. The base flow is constructed by means of a linear filter. The filter separates the radiating and non-radiating parts of the flow.

The filter can take different forms. A differential filter, taking the form of the d'Alembertian operator has been tested on a parallel flow problem. It removes the radiating components from the base flow but modifies the hydrodynamic components significantly. This undesirable property would have to be corrected in order to employ such filters to obtain the sound sources. A more general family of filters, based on convolutions carried out in the frequency domain, has been studied. The flexibility offered by convolution filters was found to be necessary to select precisely the desirable components in the flow. This strategy was applied successfully to two different flows. In particular, an axisymmetric jet, forced by two unstable modes interacting non-linearly, was filtered successfully.

The filtered base flow, containing only the non-radiating components, was used to derive the sound sources. The sources were found to take the form of a quadrupole-shaped structure, oscillating backward and forward within the first 5 diameters of the jet mixing layer. The frequency content of the source was found to correlate well with that of the far field radiating field. These sources were also compared to those obtained by using a more conventional steady base flow, for which the results were more difficult to interpret physically. An improved picture of the source mechanism , in terms of source localisation and structure, was obtained through the use of a non-radiating unsteady base-flow.

Future work will focus on analysing the structure of the sound sources discovered through this work. The

procedure will be applied to other flows, including DNS of mixing-layer flows and fully turbulent jets.

Acknowledgements

We are indebted to Dr. Victoria Suponitsky and Professor Neil Sandham, who carried out the DNS simulation for the second test case used in this paper. We would like to thank Professor Paul White for his support regarding the use of Fourier transforms, Dr. Jonathan Freund for his advice on the numerical implementation of boundary conditions, and Drs. Gwenael Gabard and Richard Sandberg for many useful discussions. This project is funded by the Engineering and Physical Sciences Research Council under grant EP/F003226/1. The authors also gratefully acknowledge Rolls-Royce plc for their financial support.

References

[1]Jordan, P. and Gervais, Y., "Subsonic jet aeroacoustics: associating experiment, modelling and simulation," *Experiments in Fluids*, Vol. 44, No. 1, 2008, pp. 1–21.

[2]Lighthill, M. J., "On Sound Generated Aerodynamically. I. General Theory," *Proceedings of the Royal Society of London. Series A, Mathematical and Physical Sciences (1934-1990)*, Vol. 211, No. 1107, 1952, pp. 564–587.

[3]Lilley, G., "On the noise from jets," *AGARD Conference Proceedings No.131 on Noise Mechanisms*, Brussels, Belgium, 1974, pp. 13 – 1.

[4]Cabana, M., Fortun, V., and Jordan, P., "Identifying the radiating core of Lighthill's source term," *Theoretical and Computational Fluid Dynamics*, Vol. 22, No. 2, 2008, pp. 87 – 106.

[5]Goldstein, M., "On identifying the true sources of aerodynamic sound," *Journal of Fluid Mechanics*, Vol. 526, 2005, pp. 337 – 347.

[6]Dahl, M., "Fourth Computational Aeroacoustics(CAA) Workshop on Benchmark Problems," *NASA/CP*, Vol. 212954, 2004, pp. 23–24.

[7]Tam, C. and Webb, J., "Dispersion-relation-preserving finite difference schemes for computational acoustics," *Journal of Computational Physics*, Vol. 107, No. 2, 1993, pp. 262 – 81.

[8]Sandberg, R. D. and Sandham, N. D., "Nonreflecting zonal characteristic boundary condition for direct numerical simulation of aerodynamic sound," *AIAA journal*, Vol. 44, No. 2, 2006, pp. 402–405.

[9]Agarwal, A., Morris, P. J., and Mani, R., "Calculation of sound propagation in nonuniform flows: Suppression of instability waves," *AIAA Journal*, Vol. 42, No. 1, 2004, pp. 80 – 88.

[10]Sandham, N. D., Salgado, A. M., and Agarwal, A., "Jet noise from instability mode interactions," *14 th AIAA/CEAS Aeroacoustics Conference(29 th AIAA Aeroacoustics Conference)*, 2008.

[11]Stromberg, J., McLaughlin, D., and Troutt, T., "Flow field and acoustic properties of a Mach number 0. 9 jet at a low Reynolds number," *Journal of Sound and Vibration*, Vol. 72, No. 2, 1980, pp. 159–176.

[12]Suponitsky, V. and Sandham, N. D., "Nonlinear mechanisms of sound radiation in a subsonic flow," *15 th AIAA/CEAS Aeroacoustics Conference(30 th AIAA Aeroacoustics Conference)*, 2009.